MATERIALS OF POWER ENGINEERING AND RADIATION-RESISTANT MATERIALS

Damageability of the Al_2O_3 Oxide Coating on the Aluminum Substrate by Pulsed Beam Plasma and Laser Radiation

V. A. Gribkov[a,], *, A. S. Demin[a], N. A. Epifanov[a], E. E. Kazilin[a], S. V. Latyshev[a], S. A. Maslyaev[a], E. V. Morozov[a], I. P. Sasinovskaya[a], V. P. Sirotinkin[a], K. N. Minkov[a], and M. Paduch[b]

[a]*Baikov Institute of Metallurgy and Material Science, Moscow, 119334, Russia*
[b]*Institute of Plasma Physics and Laser Microfusion, Warsaw, 01-497, Poland*
*e-mail: gribkovv@rambler.ru

Abstract—The following investigation of the damageability of the Al_2O_3 oxide ceramic coating on the aluminum substrate under the influence of the concentrated energy fluxes of different nature and pulse duration performed: pulsed laser radiation in the free running mode (at the power density of $q = 10^5 - 2 \times 10^6$ W/cm^2 and pulse duration of $\tau_i = 0.7$ ms) and modulated Q-switched mode ($q = 10^7 - 10^8$ W/cm^2, $\tau_i = 80$ ns), as well as the beam-plasma influence at $q = 10^7 - 10^9$ W/cm^2, $\tau = 50 - 100$ ns. It is shown that, under the influence of laser radiation within the millisecond and nanosecond ranges of the pulse impact on a semitransparent ceramic coating, the partial destruction and peeling of the ceramic layer from the metal substrate is observed. The mechanisms of the observed damageability are determined. The threshold values of the laser radiation flux at which the coating is damaged, caused by peeling, are experimentally estimated. The distribution of the temperature in the surface layer of the samples was calculated by numerical simulation, and it was shown that during laser irradiation the temperature reaches its maximum values at the depth corresponding to the contact area between the coating and substrate. It was established that the impact on the aluminum samples with the ceramic coating from the fast deuterium ion fluxes and high temperature deuterium plasma in the plasma focus device results in melting and partial evaporation of the coating surface layer; but in this case, no cracking or peeling from the aluminum substrate is observed.

Keywords: oxide ceramic coating, aluminum substrate, laser radiation, ion and plasma flux

DOI: 10.1134/S2075113319020151

INTRODUCTION

Aluminum oxide ceramic possesses high strength, hardness, and thermal and corrosion resistance [1, 2]; it is widely applied as the protective coating for the energy-loaded parts used in the machine industry, electric power industry, and space and radiation engineering. The Al_2O_3 based oxide coatings are considered in the fusion power industry as an advanced coating intended for application in the structural elements of the blanket module connector in the international thermonuclear experimental reactor ITER. Such coatings in the blanket operate under conditions of the pulsed radiation, thermal, and mechanical loads and they should have both high electrical and thermal-insulating properties as well as tribological and corrosion properties [3–8]. In addition, along with the boron nitride BN, Al_2O_3 ceramic is considered as an advanced material for the coating of the antenna rings placed inside the discharge chamber of the spherical tokamak MAST (Mega Ampere Spherical Tokamak) [9, 10].

Different sources of concentrated energy fluxes are used for investigation of the radiation and thermal resistance of the coatings: electron beams, laser radiation, fluxes of ions and plasma, etc. During the impact of the electromagnetic radiation on the compositions containing a ceramic coating and metal substrate, it is necessary to take into account the ability of the ceramic layer to pass a considerable part of the incident energy flux in a wide range of wavelengths. Peculiarities of the radiation and thermal damageability of massive ceramic samples based on aluminum oxide under the influence of the strong pulse fluxes of ions, plasma, and laser radiation are presented in [11].

The aim of this work is a comparative analysis of the damageability specifics of a ceramic coating based on the Al_2O_3 oxide developed on an aluminum substrate under pulsed laser irradiation within the millisecond and nanosecond ranges of the pulse duration and under the impact of the fast deuterium ion fluxes and high temperature deuterium plasma in the plasma focus device (PF).

Table 1. Irradiation conditions in the PF-6 device

Sample	Distance of sample from anode, cm	Power density of the ion flux q, W/cm^2, during pulse duration		Number of pulsed impacts, N	Loss of mass per pulse, mg
		50 ns	100 ns		
AL2	8	10^9	10^8	2	0.26
AL3	14	10^8	10^7	1	0.28
AL4	14	10^8	10^7	3	0.26
AL5	14	10^8	10^7	7	0.14

MATERIAL, IRRADIATION CONDITIONS, AND METHODS OF INVESTIGATION

The irradiated samples represented a flat massive aluminum substrate 4 mm thick, with the coating based on the Al_2O_3 oxide, with the structure of the γ phase grown by the electrical oxidation method (anode oxidation) of aluminum [12]. The coating thickness was about 20 μm. The pulsed laser irradiation was performed with the use of the GOS-1001 device with the radiation wavelength of λ = 1.064 μm. The pulse duration in the free generation (FG) mode was τ(FG) = 700 μs; in the modulated Q-switched (MQ) mode, it was τ(MQ) = 80 ns. The radiation was focused in such a way that the incident power density on the sample surface varied from 10^5 to 2×10^6 in the FG mode and from 10^7 to 10^8 W/cm^2 in the MQ mode. The treatment by the ion and plasma fluxes was carried out with the use of the PF device PF-6 (Warsaw, Poland). Samples were placed in the cathode part of the discharge chamber of the device. The irradiation conditions are presented in the Table 1. Irradiation of all samples during experiments was conducted on the coating side.

After irradiation, the samples were analyzed by metallographic methods with the use of a NEO-PHOT-32 optical microscope and Leica DCM 3D confocal microscope. The X-ray phase composition of the surface layer was analyzed by the methods of the X-ray diffractometry with the use of a Rigaku (XRD) Ultima-IV diffractometer (Japan). The temperature distribution in the direction normal to the irradiated surface was calculated on the basis of a 1D model similar to one described in [13]. The laser radiation absorption ratio in the ceramic coating was taken as μ = 0.0025 cm^{-1} [14].

RESULTS AND DISCUSSION

Impact of Laser Radiation

Surface microstructure. Weighing of samples before and after the pulsed irradiation showed that, regardless of the irradiation mode, their mass within the accuracy of measurements (0.05 mg) during irradiation with a low flux did not change. In the case of exceeding a certain threshold power density value of the laser radiation, cracking and partial peeling of the ceramic coating from the aluminum substrate is observed. Figure 1 shows the structure of the surface of samples after irradiation in the FG mode with the energy flux within the interval of $q = 5.5 \times 10^5 - 1.7 \times 10^6$ W/cm^2. Quite a large area of the melted aluminum surface is observed in the central part of the irradiated spot with the power density of laser radiation of 1.7×10^6 W/cm^2 (Fig. 1a).

With lower q values, after peeling of the oxide coating, sections of the Al substrate without surface melting are observed (Figs. 1b and 1c).

Figure 2 shows the structure of the samples surface after irradiation by the laser pulses in the Q-switched mode with a power density of $5 \times 10^7 - 10^9$ W/cm^2. Here, as after irradiation in the FG mode, open areas of Al surface, with the full peeling of the ceramic coating, are seen (Fig. 2a).

In addition, under the impact of laser radiation on the Al_2O_3/Al material in the MQ mode with the maximum power density of $q = 10^8$ W/cm^2, areas with partial local melting of the aluminum substrate (Fig. 2b) are observed after removal of the coating on the surface of the target sample.

Figure 3 shows the area of the irradiated surface of the oxide coating after the impact of laser radiation on the sample of the Al_2O_3/Al material in the MQ mode obtained by the method of confocal microscopy. It is seen that the coating is not observed on a large area, which indicates the possible dispersion of the coating particles after destruction and peeling. Figure 4 shows the profilometry curve of the surface relief in the zone of the coating separation from the substrate. Analysis showed that the characteristic depth of "ribbing" of the coating (the distance between the maximum and minimum values of the relief level) is several microns. The corresponding value for the Al substrate after irradiation is higher—about 10 μm.

Temperature distribution in the surface layer after the impact of laser radiation in the FG mode. Figure 5 shows diagrams of the temperature changes over the depth of samples of the Al_2O_3/Al oxide developed on the basis of the numerical calculations for different time moments after laser irradiation of the material in
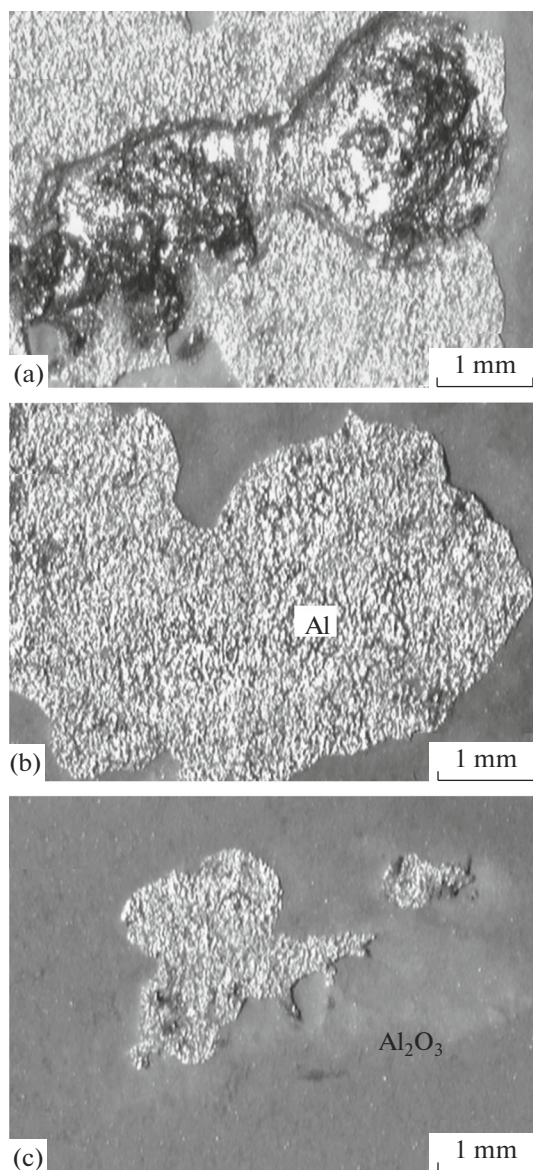
Fig. 1. Surface of the Al₂O₃/Al sample after exposure to laser radiation in the FG mode at different power densities q, W/cm²: (a) 1.7×10^6; (b) 1.1×10^6; (c) 5.5×10^5.
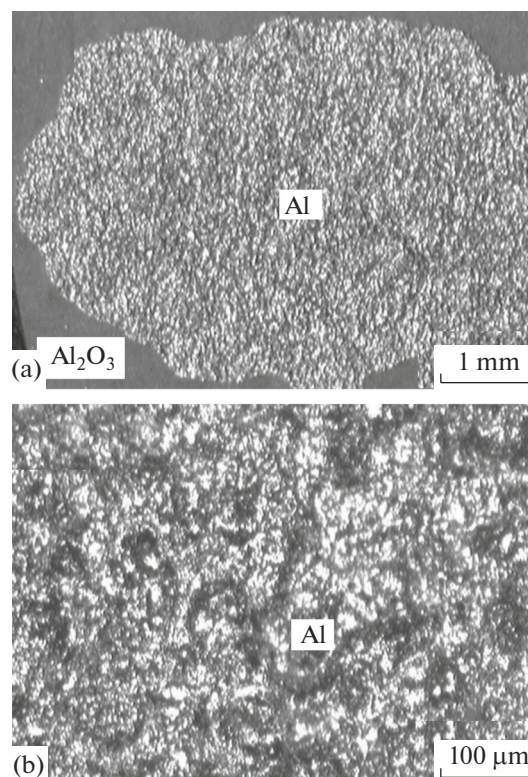

Fig. 2. Surface of the Al₂O₃/Al sample after laser irradiation in the Q-switched mode: (a) general view of the irradiated area at $q = 5 \times 10^7$ W/cm²: the Al₂O₃ coating (on the periphery of the image) and the Al spot after the coating peeling are observed in the central part of the irradiation area; (b) the Al surface with traces of local melting at the place of coating peeling ($q = 10^8$ W/cm²).

the FG mode. It is seen that, in the contact zone of the substrate and coating (at the depth of about 20 [mu]m from the surface), the maximum temperature is observed . This is connected with the fact that the analyzed ceramic is semitransparent to laser radiation with the wavelength of $\lambda = 1.06$ μm and part of the energy during pulsed laser impact goes through the coating without absorption and is emitted in the area of its contact with the surface of the aluminum substrate. The value of the maximum temperature depends on the energy flux and may exceed the aluminum melting temperature (660°C). In this case, the gradient temperature near the "surface–substrate" interface reaches 2×10^6 K/m.

With the pulse laser irradiation in the MQ mode, when the pulse time is four orders of magnitude less and radiation intensity is two orders of magnitude higher than the pulse in the FG mode, the selective heating of the area of contact of the oxide coating with the Al substrate results in a more pronounced temperature maximum (Fig. 6), and the temperature gradient near the interface boundary of the considered phases reaches values about 10^8 K/m.

Aluminum melting is accompanied by the marked increase in its specific volume (density of the melted Al, $\rho = 2.35$ g/cm³, is less than the solid-phase $\rho = 2.7$ g/cm³ [15]) with the formation of the surface wave relief and deformation and partial destruction of the coating. At the stage of the melt hardening, the high temperature gradient creates significant thermal stresses in the contact area of the aluminum oxide with the substrate, which contributes to cracking and peeling of the ceramic coating.

The threshold values of the power density q_{crit}, accompanied by peeling and destruction of ceramic coating, were determined by calculations of the tem-
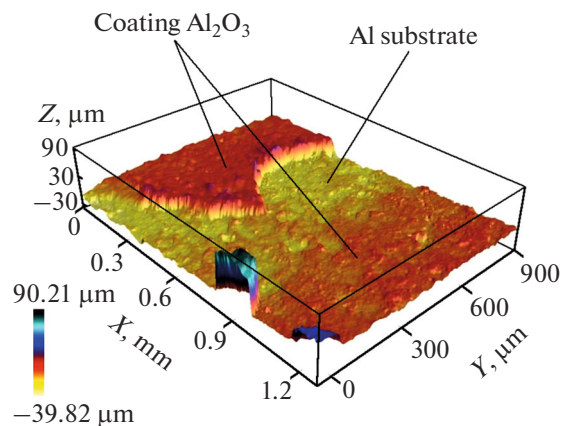
Fig. 3. Part of the Al$_2$O$_3$/Al sample of ~1200 × 900 μm after laser irradiation in the Q-switched mode with the partially destroyed and peeled ceramic coating (confocal microscopy).
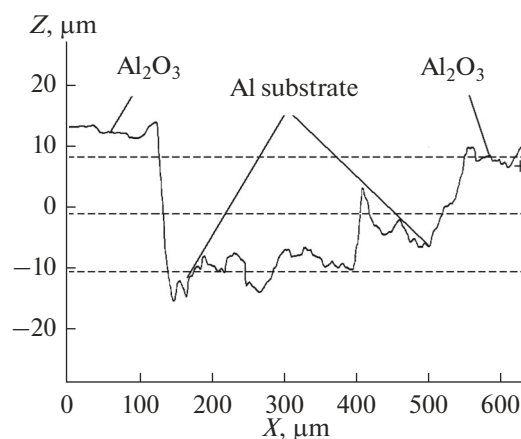

Fig. 4. The profile curve at the boundary of the "oxide coating–Al substrate" crater formed after the laser irradiation in the Q-switched mode and removal of the coating area (confocal microscopy).
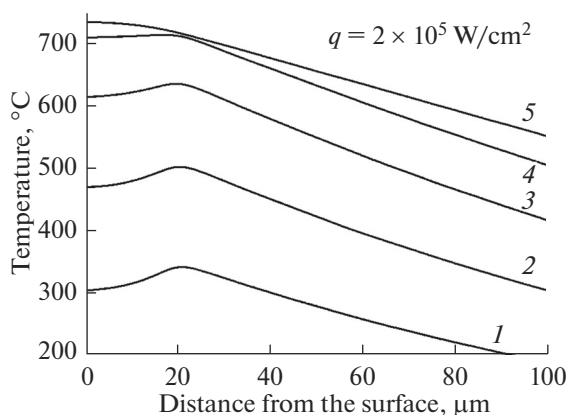

Fig. 5. Temperature distribution over the depth of the surface layer of the Al$_2$O$_3$/Al sample for different times from the onset of a laser pulse in the FG mode, μs: (*1*) 300, (*2*) 400, (*3*) 500, (*4*) 600, (*5*) 700, with the power density $q = 2 \times 10^5$ W/cm^2.
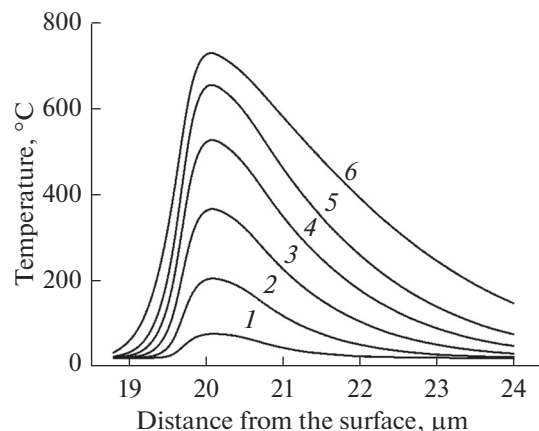

Fig. 6. Temperature distribution in the area of contact of ceramic coating with aluminum substrate for different times under laser irradiation in the Q-switched mode, ns: (*1*) 10; (*2*) 20; (*3*) 30; (*4*) 40; (*5*) 50; (*6*) 60; pulse duration of 80 ns; power density $q = 10^7$ W/cm^2.

perature change in the surface layer (SL) of the Al$_2$O$_3$/Al material and analysis of the irradiated target samples. For irradiation in the millisecond range of pulse duration in the FG mode, this value was $q_{crit} \sim 10^5$ W/cm^2, and for the nanosecond pulses in the MQ mode, $q_{crit} \sim 10^7$ W/cm^2.

Numerical modeling of the shock-wave impact. For evaluation of the possible impact of the shock wave (SW) during irradiation of the Al$_2$O$_3$/Al LI samples in the MQ mode on destruction and peeling of the ceramic coating, the calculation of the SW generation similar [16] to the state equation from [17], for the conditions of the plane geometry of the experiment for aluminum irradiation through the oxide coating layer, was made. In this case, the oxide coating in relation to the aluminum substrate was considered as the con-

densed medium with a low coefficient of the laser radiation absorption.

Analytical evaluation of the SW pressure amplitude during irradiation of the target through the condensed medium was proposed in [18]:

$$p = \sqrt{\frac{\gamma - 1}{\gamma} \frac{q_0 \rho_0 D_0}{1 + \dfrac{\rho_0 D_0}{\rho_C D_C}}}, \qquad (1)$$

where ρ_0, D_0, and ρ_C, D_C are the density and velocity of the SW front for the target material and condensed medium, respectively, and γ is the adiabatic value.

The SW in the target material was numerically modeled in this work with the maximum possible pressure amplitudes which are implemented if irradia-
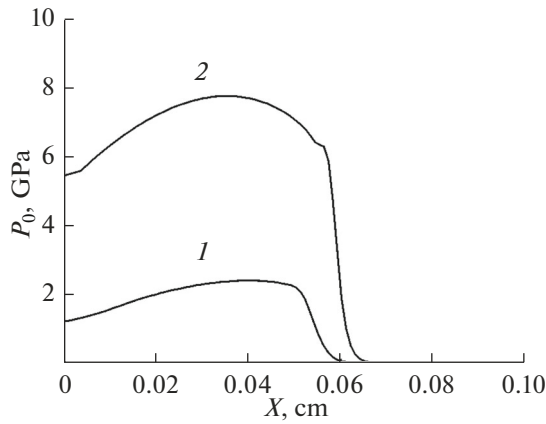
Fig. 7. Distribution of the amplitude of shock wave pressure over the depth of Al sample after laser irradiation in the Q-switched mode with power density q, W/cm^2: (*1*) 10^8, (*2*) 10^9.
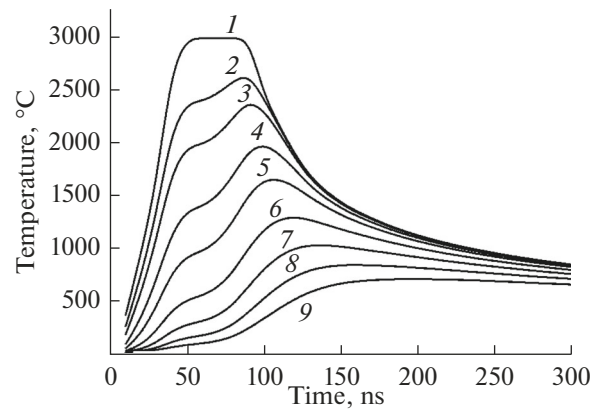

Fig. 8. Temperature distribution in the suface layer of the oxide ceramic coating on the aluminum sample under the pulsed impact of the ion-plasma flow in the Plasma Focus device at a power density of $q = 10^7$ W/cm^2 and pulse duration of 100 ns. Distance from the surface, μm: (*1*) $x = 0$; (*2*) $x = 0.05$; (*3*) $x = 0.1$; (*4*) $x = 0.2$; (*5*) $x = 0.3$; (*6*) $x = 0.45$; (*7*) $x = 0.6$; (*8*) $x = 0.75$; (*9*) $x = 0.9$.

tion is conducted through the condensed medium with the wave impedance of $Z_C = \rho D_C \rightarrow \infty$:

$$P_{max} = \sqrt{\frac{\gamma - 1}{\gamma} q_0 \rho_0 D_0}. \qquad (2)$$

In the numerical calculation, the condensed medium with the wave impedance of $Z_C = \infty$ was replaced by the state of the target boundary immobility. It was considered that laser irradiation is absorbed in the thin skin layer of the target material; the layer thickness varied within the range of $0.1-1$ μm; in this case, the change in results was insignificant.

From (1) and (2), it follows that consideration of the impact of the real condensed medium should be calculated by the following formula:

$$P = \frac{P_{max}}{\sqrt{1 + \dfrac{\rho_0 D_0}{\rho_C D_C}}}. \qquad (3)$$

The results of calculation of the distribution of the SW pressure amplitude in the cold material as at the end of the laser radiation pulse are shown below in Fig. 7 and Table 2.

It is seen that results of the numerical modeling are in good accord with the formula (2). The real SW ampli-

tude in Al, recalculated according to the formula (3), with the implemented value of $q = 10^8$ W/cm^2, is $P \approx 2.0-2.1$ GPa ($\rho = 2.69$ g/cm^3, $D_0 = 6$ km/s, $\rho_C = 3.97$ g/cm^3, $D_C = 10$ km/s [17]).

The impact of such pressure on the coating, in combination with the thermal stresses appearing in the area of the considered contact during decrease in the temperature after its pulsed step under the influence of laser radiation, leads to the observed destruction and peeling of the coating particles from the substrate. Evaluations showed that, during separation of the Al_2O_3 oxide from the Al base, the separation velocity of the destructed oxide coating particles of up to 10 μm may reach about 10 km/s.

PLASMA-BEAM IMPACT IN THE PLASMA FOCUS DEVICE

Microstructure and Thermal Heating of the Oxide Coating

During irradiation of the Al_2O_3/Al samples in the PF device at $q = 10^7 - 10^9$ W/cm^2 and $\tau_i = 50-100$ ns (Table 1), i.e., under the conditions close to the conditions of the laser impact in the MQ mode, the character of the energy absorption in the material is signifi-

Table 2. Parameters of the laser irradiation of the Al_2O_3/Al sample in the Q-switched mode and the maximum shock-wave pressure

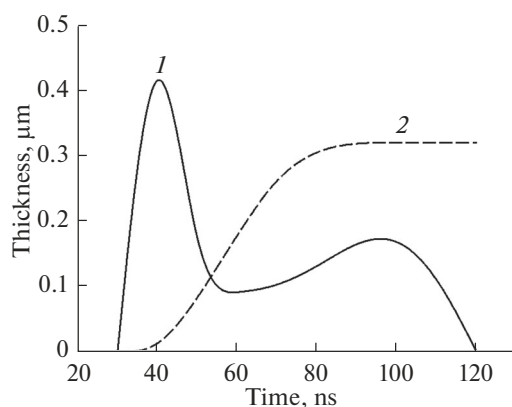| Target	Power density, q, W/cm^2	Pulse duration, τ, ns	Maximum pressure of the shock wave, P_{max}, GPa	
			numerical modeling	evaluation by formula (2)
Al	10^8	100	2.4	2.5
Al	10^9	100	7.7	8.0

Fig. 9. Change in the thickness of the melted (*1*) and evaporated (*2*) layers of ceramic coating on the aluminum sample under the pulsed impact of the ion-plasma flow with a power density of $q = 10^7$ W/cm^2 and pulse duration of 100 ns.
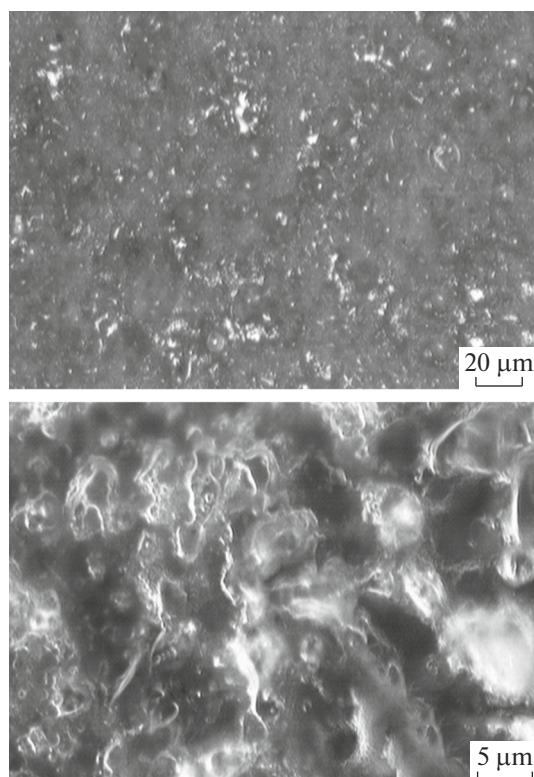

Fig. 10. Surface of the ceramic coating of the AL4 sample after impact of three pulses of deuterium ions and deuterium plasma in the PF-6 device at $q = 10^7 - 10^8$ W/cm^2.

Fig. 11. X-ray diffraction patterns for the Al$_2$O$_3$/Al oxide: (a) in the initial state; (b) after laser irradiation in the free generation mode; (c) in the Q-switched mode.

cantly different—and the flux of the implanted fast deuterium ions and high temperature deuterium plasma are absorbed in the thin surface layer of the ceramic coating having a thickness of not less than 1 μm and heat it up to high temperatures (Fig. 8). This leads to melting and erosion of the heated oxide SL owing to its partial evaporation, which was registered during weighing of samples and before and after pulsed impact of energy (Table 1). The numerical evaluations made by the methods presented in [13]
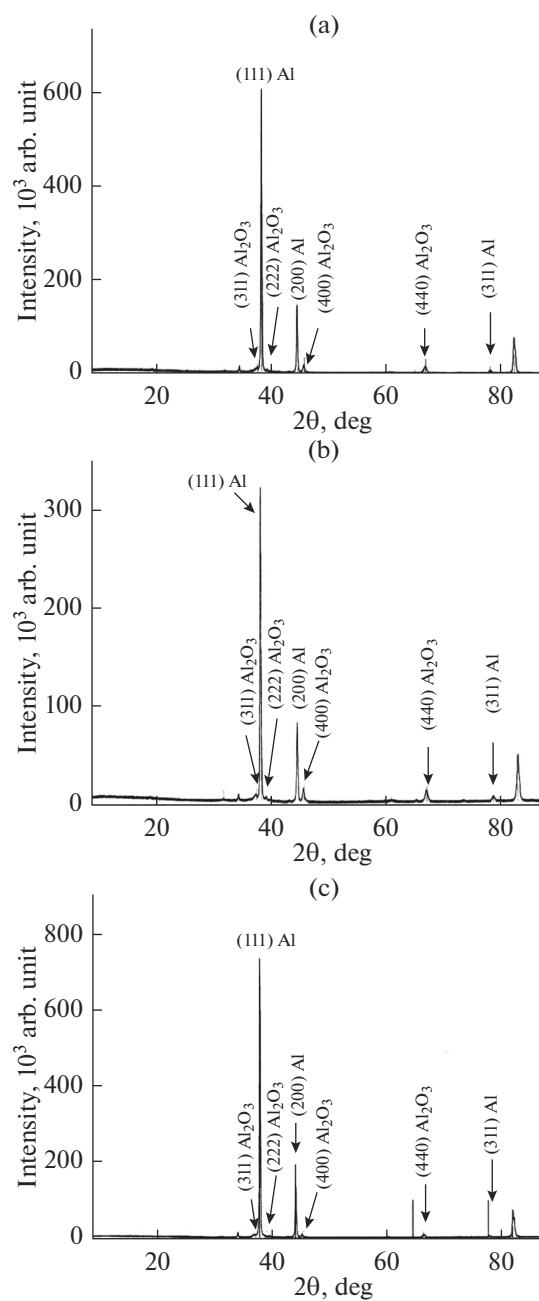
showed that, during the liquid phase (about 90 ns), the coating layer of about 0.3 μm (Fig. 9) evaporated. It is important that, with the implemented modes of the beam-plasma treatment of the material in the PF device, shock-wave impact on the coating did not arise and separation of the ceramic coating from the substrate was not observed, in contrast to the laser irradiation experiments.

Figure 10 shows the surfaces of the AL4 sample (Table 1) after its irradiation in the PF-6 device by

three pulsed impacts of fast deuterium ions and deuterium plasma. Analysis showed that the microstructure of the coating surface does not contain cracks, traces of peeling, or other macro-damage. Only wavy relief of the surface and drop-shaped fragments are observed. In addition, conspicuous is the fact that, with the growth of the number of the pulsed impacts N from 1 to 7, the fall of the mass of the irradiated material per one pulse decreases by a factor of two (Table 1). This may be the result of precipitation of the oxide copper coating on the surface (anode material) and elements of the working chamber of the PF device, evaporating during pulsed discharges [19, 20]. The results show that, with the increase in the number N, the mass gain of the target material sample due to precipitation of elements on the oxide coating dominates the mass loss due to partial evaporation of the oxide surface layer.

X-ray Phase Analysis

Figures 11 and 12 show the X-ray diffraction patterns in the initial state and after the pulse laser and beam-plasma impacts. The most intense lines on the X-ray diffraction patterns refer to aluminum; the lines of the low intensity correspond to the Al$_2$O$_3$ oxide. As is seen from Figs. 11 and 12, the general character of the X-ray diffraction patterns remained practically the same after the experiments on irradiation of the samples by the ions and plasma fluxes. In this case, the intensity ratio of the Al lines and Al$_2$O$_3$ oxide on the X-ray diffraction patterns, after the laser impact in the FG mode and beam-plasma irradiation in the PF (Figs. 11b and 12), is close to the corresponding values for the target sample in the initial state (Fig. 11a). At the same time, after the impact of laser radiation on the material in the MQ mode (Fig. 11c) the lines of the Al$_2$O$_3$ oxide became vanishingly weak, which is connected with the partial peeling of the oxide coating from the Al substrate.

CONCLUSIONS

Investigation of the damageability of the ceramic coating on the basis of the Al$_2$O$_3$ oxide developed on the surface of the aluminum substrate under the influence of concentrated laser energy fluxes of different nature and pulse duration was performed: pulsed laser radiation in the free generation mode (with the power density of $q = 10^5 - 2 \times 10^6$ W/cm^2 and pulse duration of $\tau_i = 0.7$ ms) and modulated Q-switched mode ($q = 10^7 - 10^8$ W/cm^2, $\tau_i = 80$ ns), as well as beam-plasma impact at $q = 10^7 - 10^9$ W/cm^2, $\tau = 50 - 100$ ns.

It was shown that the considered coating is semi-transparent to laser radiation with the wavelength of $\lambda = 1.06$ μm, and the impact of this radiation on the Al$_2$O$_3$ ceramic in the millisecond and nanosecond range of pulse duration results in peeling of the ceramic layer from the substrate.
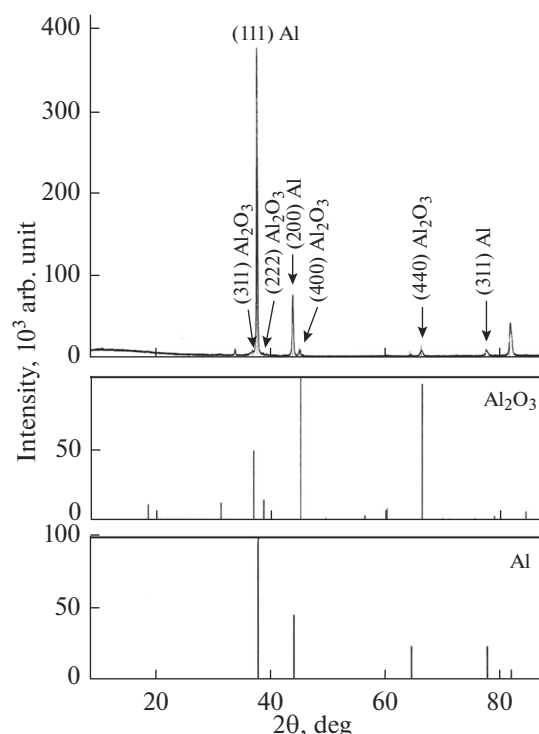

Fig. 12. X-ray diffraction patterns for the Al$_2$O$_3$/Al oxide after the beam-plasma impact in the PF device (3 pulses) and reference lines for pure Al and Al$_2$O$_3$.

The mechanisms of the observed peeling, primarily connected in the free generation mode with the melting of the aluminum substrate and impact of thermal stresses in the area of the contact of the coating with the substrate and in the modulated Q-switched mode mainly with the shock-wave impact appearing in the contact area, were determined.

The threshold values of the power density of the pulsed laser radiation accompanied by the destruction and partial peeling of the coating were experimentally evaluated: in the free generation mode, the above damageability starts at $q \sim 10^5$ W/cnm^2; in the modulated Q-switched mode, at $q \sim 10^7$ W/cnm^2. The distribution of the temperature and the amplitude of the shock wave in the surface layer of the target samples was calculated by the numerical modeling method. It was shown that the temperature distribution under the impact of laser radiation, both in the free generation mode and in the modulated Q-switched mode has a nonmonotonic character, where the temperature reaches the maximum values at the depth corresponding to the contact area of the coating with the substrate. The shock-wave impact in this area appearing during laser irradiation in the modulated Q-switched mode is sufficient for separation of the ceramic coating from the aluminum substrate.

It was established that the impact on the aluminum samples with the ceramic coating based on Al$_2$O$_3$ of

fast deuterium ion fluxes ($E = 100$ keV) and high temperature deuterium plasma in the plasma focus device results in melting and partial evaporation of the coating surface layer; but in this case cracking, peeling, and other micro-damage of the ceramic layer on the surface of the aluminum samples are not observed.

As a whole, the above experiments and investigations showed that the ceramic coating made of Al_2O_3 oxide on the aluminum substrate appeared to be more resistant to the strong beam-plasma impacts of the nanosecond pulse duration range implemented in the Plasma Focus device as compared with pulsed laser irradiation with the wavelength of 1.064 μm both in the free generation mode and in the modulated Q-switched mode.

ACKNOWLEDGMENTS

REFERENCES

1. Aruna, S.T., Balaji, N., Shedthi, J., and Grips, V.K.W., Effect of critical plasma spray parameters on the microstructure, microhardness and wear and corrosion resistance of plasma sprayed alumina coatings, *Surf. Coat. Technol.*, 2012, vol. 208, pp. 92–100.

2. Bandyopadhyay, P., Chicot, D., Venkateshwarlu, B., Racherla, V., Decoopman, X., and Lesage, J., Mechanical properties of conventional and nanostructured plasma sprayed alumina coatings, *Mech. Mater.*, 2012, vol. 53, pp. 61–71.

3. Hodgson, E.R. and Shikama, T., Radiation effects on the physical properties of dielectric insulators for fusion reactors, *Compr. Nucl. Mater.*, 2012, vol. 4, pp. 701–724.

4. Rodchenkov, B.S., Ivanov, V.M., Kalinin, G.M., Kozlov, A.V., Strebkov, Yu.S., and Scherbakov, E.N., Neutron irradiation effects on properties of insulator coating for ITER in-vessel components, *J. Nucl. Mater.*, 2004, vols. 329–333, nos. 1–3, pp. 1486–1489.

5. Ibarra, A. and Hodgson, E.R., The ITER project: the role of insulators, *Nucl. Instrum. Methods Phys. Res., Sect. B*, 2004, vol. 218, nos. 1–4, pp. 29–35.

6. Shikama, T., Knitter, R., Konys, J., Muroga, T., Tsuchiya, K., Moesslang, A., Kawamura, H., and Nagata, S., Status of development of functional materials with perspective on beyond-ITER, *Fusion Eng. Des.*, 2008, vol. 83, nos. 7–9, pp. 976–982.

7. Zaitsev, A.N., Yagopol'skii, A.G., and Aleksandrova, Yu.P., Influence of structure and chemical composition of plasma-sprayed coatings on their adhesive and tribological properties, *Izv. Vyssh. Uchebn. Zaved., Mashinostr.*, 2014, no. 12, pp. 53–62.

8. Raffray, A.R. and Merola, M., Overview of the design and R&D of the ITER blanket system, *Fusion Eng. Des.*, 2012, vol. 87, nos. 5–6, pp. 769–776.

9. Gribkov, V.A., Tuniz, C., Demina, E.V., Dubrovsky, A.V., Pimenov, V.N., Maslyaev, S.V., et al., Experimental studies of radiation resistance of boron nitride, C2C ceramics Al_2O_3 and carbon–fiber composites using a PF-1000 plasma-focus device, *Phys. Scr.*, 2011, vol. 83, no. 4, art. ID 045606. doi 10.1088/0031-8949/83/04/045606

10. Kirk, A., Koch, B., Scannell, R., Wilson, H.R., Counsell, G., Dowling, J., Herrmann, A., Martin, R., Walsh, M., et al., Evolution of filament structures during edge-localized modes in the MAST Tokamak, *Phys. Rev. Lett.*, 2006, vol. 96, art. ID 185001.

11. Maslyaev, S.A., Morozov, E.V., Romakhin, P.A., Pimenov, V.N., Gribkov, V.A., Tikhonov, A.N., Bondarenko, G.G., Dubrovsky, A.V., Kazilin, E.E., Sasinovskaya, I.P., and Sinitsyna, O.V., Damage of Al_2O_3 ceramics under the action of pulsed ion and plasma fluxes and laser irradiation, *Inorg. Mater.: Appl. Res.*, 2016, vol. 7, no. 3, pp. 330–339.

12. Lobanov, M.L., Kardonina, N.I., Rossina, N.G., and Yurovskikh, A.S., *Zashchitnye pokrytiya* (Protective Coatings), Yekaterinburg: Ural. Gos. Univ., 2014.

13. Maslyaev, S.A., Thermal effects at pulsed radiation of materials in dense Plasma Focus device, *Perspekt. Mater.*, 2007, no. 5, pp. 47–55.

14. Lingart, Yu.K., Petrov, V.A., and Tikhonova, N.A., Optical properties of leucosapphire at high temperatures. I. Translucency area, *Teplofiz. Vys. Temp.*, 1982, vol. 20, no. 5, pp. 872–880.

15. *Fizicheskie velichiny. Spravochnik* (Physical Values: Handbook), Grigor'ev, I.S. and Meilikhov, E.Z., Eds., Moscow: Energoatomizdat, 1991.

16. Latyshev, S.V., Gribkov, V.A., Maslyaev, S.A., Pimenov, V.N., Paduch, M., and Zielinska, E., Generation of shock waves in materials science experiments with dense plasma focus device, *Inorg. Mater.: Appl. Res.*, 2015, vol. 6, no. 2, pp. 91–95.

17. Zel'dovich, Ya.B. and Raizer, Yu.P., *Fizika udarnykh voln i vysokotemperaturnykh gidrodinamicheskikh yavlenii* (Physics of Shock Waves and High-Temperature Hydrodynamic Phenomena), Moscow: Nauka, 1966.

18. Ivanov, L.I., Nikiforov, Yu.N., and Yanushkevich, V.A., The effect of changes in the electrical conductivity of semiconductor crystals under a shock wave from the pulsed radiation of optical quantum generators, *Zh. Eksp. Teor. Fiz.*, 1974, vol. 67, no. 7, pp. 147–149.

19. Morozov, E.V., Maslyaev, S.A., Pimenov, V.N., Gribkov, V.A., Demina, E.V., Sasinovskaya, I.P., Bondarenko, G.G., and Gaidar, A.I., Evolution of tungsten surface affected by powerful energy fluxes, *Perspekt. Mater.*, 2015, no. 10, pp. 32–45.

20. Vali, B., Laas, T., Paju, J., Shirokova, V., Paduch, M., Gribkov, V.A., Demina, E.V., Pimenov, V.N., Makhlai, V.A., and Antonov, M., The experimental and theoretical investigations of damage development and distribution in double-forget tungsten under plasma irradiation-initiated extreme heat loads, *Nukleonika*, 2016, vol. 61, no. 2, pp. 169–177. doi 10.1515/nuka-2016-0029

Translated by E. Grishina